Nucleobindin-1 *(Nucb1)* disruption affects feeding, metabolism, and glucose homeostasis in mice in an age-, sex-, diet- and light cycle-dependent manner

Atefeh Nasri[1], Emilio J Vélez[1,2], Jithine Jayakumar Rajeswari[1], Azadeh Hatef[1], Suraj Unniappan[1]

[1]Laboratory of Integrative Neuroendocrinology, Department of Veterinary Biomedical Sciences, Western College of Veterinary Medicine, University of Saskatchewan, Saskatoon, Saskatchewan S7N 5B4, Canada

[2]Present address: Université de Pau et des Pays de l'Adour, E2S UPPA, INRAE, UMR1419 Nutrition Métabolisme et Aquaculture, Saint-Pée-sur-Nivelle, 64310, France

Corresponding Author:
Dr. Suraj Unniappan
Department of Veterinary Biomedical Sciences
Western College of Veterinary Medicine
University of Saskatchewan
52 Campus Drive
Saskatoon, Saskatchewan S7N 5B4
Canada
Tel: 1-306-966-7414
Fax: 1-306-966-7376
E-mail: suraj.unniappan@usask.ca

Abstract

Background: Nesfatin-1 (NESF-1), encoded in the calcium and DNA binding protein (Nucleobindin 2, NUCB2) is an orphan ligand with metabolic effects. Recently, our lab provided evidence for a NESF-1-like peptide (NLP) in a NUCB2-related precursor, NUCB1, in zebrafish and rodents. This research aims to determine whether endogenous NUCB1 is critical for energy homeostasis.

Methods and Main Findings: Global genetic disruption of *Nucb1* (*Nucb1* knockout/KO mice) led to increased food intake in chow-fed male and female mice across different points of light and dark phases. A similar increase in water intake was seen in female *Nucb1* KO mice but not in males. White adipose tissue weight was significantly increased in male and female *Nucb1* KO mice. Dark phase total activity was increased in male *Nucb1* KO mice, while it was decreased in female *Nucb1* KO mice compared to wildtype littermates. Energy derived from carbohydrates was raised during the dark phase; while energy derived from fat was significantly decreased in both male and female *Nucb1* KO mice. Male *Nucb1* KO mice were lighter in the early stages, but these differences disappeared as they aged. Meanwhile, no differences in bodyweight were observed in female *Nucb1* KO mice. Male *Nucb1* KO mice handled glucose better during an oral glucose tolerance test, while the opposite effect was found in an intraperitoneal (IP) glucose tolerance test. The above results from chow-fed mice were largely true in 10% and 60% fat diet-fed mice. A significant two-way interaction between mice group and time was observed on weekly food intake of male and female *Nucb1* KO mice fed control fat diet, but not in 60% fat-fed group. Handling of blood glucose during IPGTT was better in male *Nucb1* KO mice fed both diets, while such an effect was not observed in female KO mice. A significant two-way interaction of mice group and time on food and water intake value in 24 h was observed for male *Nucb1* KO mice fed 10% fat diet. The total physical activity during the dark phase and energy expenditure during the light phase showed a sex-specific pattern in male and female *Nucb1* KO mice fed 10% fat diet. Energy expenditure showed a sex-specific pattern in *Nucb1* KO mice during the dark phase. Moreover, adiposity increased in male *Nucb1* KO mice fed a high fat diet.

Conclusions: Our results indicate that the disruption of *Nucb1* leads to metabolic changes *in vivo*. The phenotype appears to depend on sex, age, diet, and the light-dark cycle. In conclusion, these

outcomes furnish important evidence supporting critical roles for endogenous NUCB1 in energy homeostasis.

Keywords: Nucleobindin-1, Nesfatin-1, Nesfatin-1-Like-Peptide, Metabolism, Glucose Homeostasis, Mice.

1. Introduction

Nucleobindin-1 (NUCB1) is a calcium and DNA binding protein that was originally reported in 1990. The peptide has both DNA and calcium-binding EF-hands [1, 2]. NUCB1 is a secreted peptide [3, 4], which is detected in many tissues in mammals, especially in humans and rodents [5, 6]. This peptide has been implicated in several biological processes, including calcium homeostasis [7], regulation of DNA [8], neuronal biology [9], hormone secretion, and protein folding [10]. These functions clearly place NUCB1 as an important mediator of cellular and physiological processes in mammals. Years later, another peptide was named nucleobindin 2 (NUCB2) due to its structural similarity with NUCB1 [11]. NUCB2 has calcium and DNA binding sites and is a secreted protein [1]. More recently, Oh-I and colleagues identified a bioactive peptide within NUCB2 that causes satiety and fat loss in rats and named it nesfatin-1 (NESF-1) [12]. Through immunoprecipitation and mass spectrometry, our lab discovered that a NESF-1-like peptide (NLP) is processed from NUCB1 [13]. Further research found that NLP is an anorexigenic peptide in rats [14] and goldfish [11] and has insulinotropic actions in mice [10]. We previously reported that NLP suppressed the basal and thyrotropin-releasing hormone (TRH)-induced prolactin expression in rat GH3 somatolactotrophs [15]. Moreover, NLP reduced growth hormone (GH) synthesis and secretion from rat somatotrophs while stimulated the synthesis of proopiomelanocortin (POMC) in mouse corticotrophs. This direct action of NLP on GH and POMC was mediated via the cAMP response element-binding protein (CREB) pathway [16]. Moreover, fluorescent-tagged NLP was able to bind to the surface of rat somatotrophs. These suggest a G coupled protein receptor (GPCR) mediated action of NLP in modulating GH [16]. While these evidence from multiple species and cells studies provide clear indications that NLP is a bioactive peptide that modulates whole-body energy homeostasis and hormone secretion, whether endogenous NUCB1 is critical for homeostasis is unknown. Therefore, the main goal of research outlined in this research was to address this gap in knowledge. We hypothesized that the disruption of endogenous *Nucb1* will negatively affect whole-body energy homeostasis in mice. Both male and female mice were studied separately. Our results indicate that the disruption of *Nucb1* results in mild metabolic defects in mice, and these effects occur in a sexually dimorphic manner.

95 ## 2. Materials and Methods

96 ### 2.1. Animals

97 Breeding pairs of homozygous C57BL/6NCrl-*NUCB1*$^{em1(IMPC)Mbp}$/Mmucd, 043641-UCD
98 mice from the University of California, San Diego (generated by Dr. Kent Lloyd, Mouse Biology
99 Program, University of California-Davis, USA) were used to establish a colony of *Nucb1* disrupted
100 mice. To generate these global *Nucb1* disrupted mice, the exon 4 and flanking splicing regions of
101 *Nucb1* were constitutively deleted using CRISPR Cas9 gene editing technology in C57BL/6J
102 mouse zygotes. All the animals were housed under 12 h light:12 h dark cycle (7 AM - 7 PM),
103 humidity (30 – 60 %), and temperature (18 – 22 ºC) controlled vivarium located in the College of
104 Medicine Lab Animal Services Unit, University of Saskatchewan. All animal use and care
105 protocols were prepared based on the guidelines of the Canadian Council for Animal Care and
106 ARRIVE guidelines and they were approved by the University of Saskatchewan Animal Care
107 Committee (Animal Care Protocol # 2012-0033).

108 ### 2.2. Genotyping

109 Wildtype (WT) and knockout (KO) littermate genotypes were confirmed RT-PCR. Briefly,
110 tissue samples were collected via tail clipping and DNA was extracted using Direct PCR Lysis
111 Reagent (Cat no. 101 101 T, Viagen Biotech, USA), and 1.5 µL of the lysate from each sample
112 was used for PCR. The Taq DNA Polymerase recombinant PCR kit (Cat no. 10342-020, Thermo
113 Fisher Scientific, USA) was used following the manufacturer's protocol. For the *Nucb1* gene, pairs
114 of forward (GTTGTCTCTGTTGAGTATTGAAAGACAGG) and reverse primers
115 (GGATACGAGCTCAGGTCACCAGG) were designed by MMRRC at University of California
116 (Davis) to specifically amplify either the WT or the KO allele in separate PCR amplifications. The
117 PCR products were separated on 1.5% agarose gel, and the images were captured using the
118 ChemiDoc MP Imaging System (Bio-Rad, Canada).

119 After confirmation of the homozygous KO genotype, age-matched WT and *Nucb1* KO
120 mice for experiments were moved to the Animal Care Unit of the Western College of Veterinary
121 Medicine (University of Saskatchewan) and maintained under the same conditions. These mice
122 were used for two different studies, explained below. After finishing all experiments, pancreas
123 (whole tissue) and large intestine (transverse colon) samples were collected from each mouse after

124 euthanasia to re-confirm the genotype of each animal. In this case, total RNA was extracted, and
125 cDNA was made as mentioned below. Finally, 1 μL of cDNA of each sample was subjected to
126 PCR amplification, PCR product separation in agarose gel and imaging, as explained above.

127 **2.3. Diets**

128 The first set of studies were carried out on age-matched mice fed a standard rodent chow
129 diet (Cat no. 500I, LabDiet, 7.94% carbohydrate, 28.67% protein, 13.38% fat, Energy density =
130 4.09 Kcal/g). Second set of studies were conducted on age-matched mice fed a control fat diet (Cat
131 no. D12450B, Research Diets Inc., 70% carbohydrate, 20% protein, 10% fat, Energy density =
132 3.82 Kcal/g) and high-fat diet (Cat no. D12492, Research Diets Inc., 20% carbohydrate, 20%
133 protein, 60% fat, Energy density = 5.21 Kcal/g). The full list of ingredients for 10% and 60% fat
134 diets are provided in ***Supplementary Table 1***. Bodyweight, food intake and blood glucose of all
135 mice were weekly monitored as explained below. In addition, whole-body metabolic parameters
136 were measured using the Comprehensive Lab Animal Monitoring System (CLAMS, Columbus
137 Instruments, USA), as well as the ability to handle glucose was tested (see below). After
138 experiments were done, mice were euthanized by cervical dislocation. Bodyweight of mice was
139 noted, and liver and weight adipose tissue were weighed and collected.

140 **2.4. Food intake, blood glucose, bodyweight – weekly monitoring**

141 To determine the phenotypic changes in male and female *Nucb1* KO mice versus WT
142 littermates fed either standard chow diet or high-fat diet, blood glucose level was recorded weekly
143 after fasting mice for 4-h using glucometer for 24-25 weeks (OneTouch Ultra®, LifeScan, Canada).
144 In addition, food intake and bodyweight gain of mice were also monitored weekly using a digital
145 scale. Mice were age-matched, and the monitoring started around 10 weeks post-weaning for
146 chow-fed mice and 13 weeks post-weaning for high-fat-fed mice.

147 **2.5. Oral or intraperitoneal glucose tolerance tests (O/IPGTT)**

148 To elucidate whether genetic disruption of *Nucb1* affect orally administered or
149 intraperitoneally injected glucose tolerance, OGTT and IPGTT were performed, respectively.
150 These tests were performed (littermate controls and *Nucb1* KO mice, $n \geq 6$) in age-matched mice
151 (33-34 weeks old for chow-fed mice and 25-26 weeks old for high-fat-fed mice). All animals were
152 fasted 4 h (9 AM) before the commencement of oral gavage (OGTT) or IP administration (IPGTT)

153 at 1 PM. For OGTT, 2 g/kg bodyweight of D-Glucose (Fisher Chemical, #D16-500) dissolved in
154 sterile water (Gavage volume: 200 µL) was administered to mice using insulin syringes (BD,
155 #324911) attached to animal gavage needles (Popper and Sons, USA, #9921). For IPGTT, 2 g/kg
156 bodyweight of D-Glucose dissolved in sterile saline (injection volume: 200 µL) was administered
157 to mice using insulin syringes attached to a 27G needle in the lower right quadrant of the abdomen
158 to avoid damage to the urinary bladder, caecum, and other abdominal organs. For both tests, blood
159 glucose via tail snip was measured at time points 0, 10, 20, 30-, 60-, 90- and 120-min post-
160 administration using a glucometer. Each bleeding took 30-60 s, and mice were returned to their
161 respective cages until the next bleed. The area under the curve (AUC) was calculated using
162 GraphPad Prism Version 8.0 (GraphPad Inc., USA) [The formula (concentration of glucose at T1
163 + concentration of glucose at T2)/2·(T2-T1), where T1 and T2 are two consecutive time points].

164 **2.6. Assessment of whole-body energy homeostasis using the comprehensive lab animal**
165 **monitoring system (CLAMS)**

166 The whole-body metabolic parameters were measured in both male and female littermate
167 control and *Nucb1* KO mice using the CLAMS (Columbus Instruments, USA). Mice were
168 transferred to CLAMS cages to acclimate for 3 days before monitoring feeding, drinking, and other
169 metabolic parameters over 24 h (one dark phase and one light phase). CLAMS monitoring was
170 completed twice each on chow-fed mice (20-21 weeks old) and high-fat-fed mice (28-29 weeks
171 old), and then data from each diet group repetition were pooled from two studies (n = 4 mice/group
172 maximum tested per study) for each sex. The CLAMS system was calibrated according to the
173 manufacturer's instructions prior to beginning the experiments. This system is equipped with an
174 open-circuit calorimeter for measuring cumulative oxygen (O_2), O_2 consumption (VO_2), carbon
175 dioxide production (VCO_2), and energy expenditure (Heat). The respiratory exchange ratio (RER)
176 was calculated by dividing VCO_2 by VO_2, with values ranging from 0.7 to 1.0. A shift in RER
177 value towards 0.7 indicates that fat is the major substrate used for energy production, while a shift
178 towards 1.0 indicates that carbohydrate is the main substrate used. The percent of fat and
179 carbohydrates utilized for energy by each animal was determined from the RER. The energy
180 derived from carbohydrates or fats was extrapolated from RER data by employing the methods of
181 Mclean and Tobin [17], using the equation and methods described in the protocols provided by the
182 Columbus instruments (http://www.colinst.com). Accordingly, the equations are: energy derived
183 from carbohydrate = Percentage of carbohydrate/100 × Heat. Percentage carbohydrate values are

184 based on the RER values (RER range; % carbohydrate: 0 – 0.7285: 0; 0.7285 – 0.775: 14.7; 0.775
185 – 0.825: 31.7; 0.825 – 0.875: 48.8; 0.875 – 0.925: 65.9; 0.925 – 0.975: 82.9; Above 0.975: 100).
186 Percentage fat = 100 - % carbohydrate. Energy derived from fat = Percentage of fat / 100 × Heat.
187 Each cage is also equipped with a system of infrared (IR) beams that detect animal movement in
188 the three planes/axes (X, Y and Z). We measured the total physical activity as the sum of number
189 of activities recorded as X+Y+Z axes IR beam breaks. To adhere to the figure limits of this journal,
190 the most significant results from the CLAMS measurements are presented.

191 **2.7. RNA extraction, cDNA synthesis and qPCR**

192 Different tissues from chow-fed mice were collected, and total RNA was extracted, cDNA
193 was made, and qPCR was performed according to the published methods [18]. Briefly, tissues
194 were homogenized in 1 mL of RiboZol (Cat no. N580, VWR, USA), and then total RNA was
195 precipitated in 500 µL of isopropanol. After the final washing step with 75% ethanol twice, RNA
196 pellets were suspended in RNase-free water. The concentration of total RNA was measured using
197 the NanoDrop2000 (Thermo Fisher Scientific, USA), and RNA purity was assessed by 260/280
198 and 260/230 ratios. Total RNA (1 µg) was reverse transcribed to cDNA using an iScript cDNA
199 synthesis kit (Cat no. 170884, BioRad, USA), following the manufacturer's instructions. qPCR
200 was conducted using the CFX Connect Optic module (BioRad, USA) using SensiFAST SYBR
201 No-ROX Kit (Cat no. BIO-98050, Bioline, Froggabio, Canada). The amplification reaction
202 contained 1 µL of diluted cDNA, 0.5 µL of primer mix (forward and reverse) at 10 µM, 5 µL of
203 SYBR green PCR master mix and water up to the total volume of 10 µL. The amplification
204 efficiency for each primer set was obtained from a serial dilution of cDNAs with a dilution factor
205 of 4. Those primers with reaction efficiency of 90–110%, with a single disassociation peak of PCR
206 products and the absence of primer-dimer were considered in this study. The dilution factor of
207 cDNA samples was selected based on the best threshold cycle (CT) range for each primer set. The
208 primer sequences and their annealing temperatures are listed in ***Supplementary Table 2***. The
209 thermal cycling set-up for all genes was the following: denaturation (95 °C for 5 s), annealing
210 (specific for each primer for 25 s) and elongation (60 °C for 25 s), 35 cycles. Three negative
211 controls, including no template DNA (NTC control), no reverse transcriptase control from cDNA
212 synthesis process (RTC control), and a nuclease-free water sample (PCR control) were also

213 included for each gene. The transcript abundance was calculated based on the Pfaffl method based
214 on gene-specific efficiencies relative to the geometric means of the two housekeeping genes.

215 **2.8. Statistical analysis**

216 Two-way mixed ANOVA (mice strain [group] and time factor) was used to compare the
217 mean differences between WT and *Nucb1* KO mice on the weekly measured bodyweight, blood
218 glucose, and food intake during 24-25 weeks, as well as to compare the food and water intake
219 during 24 h in CLAMS studies. Before running the two-way mixed ANOVA, the normal
220 distribution of the data and the presence of outliers were evaluated using Shapiro-Wilk test and
221 ROUT methods, respectively. Sphericity was not assumed following the recommendation of
222 Maxwell and Delaney [19], and the Geisser and Greenhouse epsilon hat method was used to adjust
223 the results considering the epsilon value. Bonferroni's multiple comparison test was performed as
224 a *post hoc* analysis to compare the dependent variable results between mice strain (group) in each
225 time-point. Unpaired samples *t*-test was used for analyzing the differences in energy expenditure,
226 energy derived from carbohydrates or fat and total physical activity in CLAMS studies, as well as
227 to compare AUC in the glucose tolerance tests (IPGTT and OGTT). All analysis were carried out
228 using GraphPad Prism Version 8.0 (GraphPad Inc., USA) and statistical differences were
229 considered at $p < 0.05$.

230 Chow fed and high-fat-fed mice data were also analyzed using generalized estimating
231 equation (GEE) statistical method. In this test, mouse ID was considered as subject effect. The
232 time blocks/duration varied based on the nature of experiment (week/mice age for weekly
233 monitoring of bodyweight, food intake and blood glucose, hour for CLAMS as well as time point
234 for glucose tolerance tests) that was considered as within-subjects factor and as a covariate in
235 predictor section of GEE commands. The majority of predictors were binary variables, including
236 female and male for mice sex, WT and *Nucb1* KO for mice group (presence or absence of an
237 undisrupted *Nucb1* gene), light and dark phases for day phase. As mentioned above, diet is a binary
238 factor for high fat diet experiments, which have two levels, control fat diet (10% fat) and
239 experimental fat diet (60% fat). The first order of autoregressive model (AR1) was chosen as an
240 ideal working correlation matrix for all experiments. Repeated measures were assumed to have
241 AR1 relationship, which means the current values are a function of prior values plus error. This
242 assumes time series data with equal intervals. This model is a common choice in longitudinal

243 models such as time series experiments. The scale response was chosen as linear. First, the general
244 effect of predictors on dependent variables were examined and then two-, three- and four-way
245 interactions of predictors in the model were checked, respectively.

246 **3. Results**

247 **3.1. Genotyping**

248 PCR on genomic DNA provided bands of the expected size (397 bp) and confirmed the
249 disruption of *Nucb1* in homozygous mice, compared to WT littermates (611 bp) (**Figure 1A**).
250 Some samples from *Nucb2* KO mice were used to validate the results. Since the genetic disruption
251 in *Nucb2* was not within the location where primers are targeted, we expected to observe the same
252 band size as WT for this group.

253 The analysis of the intestine and pancreas showed the predicted band corresponding to the
254 397 bp in *Nucb1* mice. Although the band around 611 bp was not detected in any male or female
255 WT mice, the band corresponding to 397 bp was absent in all WT mice (**Figure 1B** and **Figure**
256 **1C**).

257 **3.2. Weekly bodyweight, food intake, and basal blood glucose monitoring**

258 *Weekly bodyweight*

259 Although the bodyweight of chow fed male *Nucb1* KO mice was initially lower than that
260 of WT littermates in the first monitoring phase (weeks 11-19), from week 20 the bodyweight has
261 normalized, and no significant differences were observed throughout the rest of the experiment
262 (**Figure 2A**). In contrast, the disruption of *Nucb1* in female mice did not affect bodyweight
263 throughout the experiment **(Figure 3A)**. No significant differences in bodyweight were found in
264 male and female *Nucb1* KO mice fed either 10% or 60% fat diet during the monitoring **(Figure**
265 **4A** and **Figure 5A)**.

266 *Weekly food intake*

267 The genetic disruption of *Nucb1* in male mice did not alter food intake during the 6-month
268 monitoring when compared to WT controls **(Figure 2B)**. Female *Nucb1* KO mice showed higher
269 food intake at some weeks **(Figure 3B)**. Hence, a significant interaction between female mice
270 groups and time was observed for food intake ($p < 0.0001$). The male *Nucb1* KO mice fed control

271 and high-fat diet did not reveal higher food intake during weekly monitoring compared to their
272 corresponding WT littermates (**Figure 4B**). Interestingly, a significant interaction between 10%
273 fat-fed male mice and time on food intake was observed ($p < 0.0001$). Although the disruption of
274 *Nucb1* in female mice fed control and high-fat diets did not alter food intake during weekly
275 monitoring (**Figure 5B**), a significant interaction between time and female mice groups on food
276 intake was observed for both control and high-fat-fed mice.

277 *Weekly basal blood glucose levels*

278 The genetic disruption of *Nucb1* in male mice did not alter the blood glucose level (**Figure**
279 **2C**). However, a significant interaction between time and male mice groups on blood glucose
280 levels was found ($p = 0.0141$). In contrast, in female mice, significant differences were found in
281 the blood glucose level at one specific point (i.e., week 13), being higher in KO mice compared to
282 the WT littermates and for week 34, blood glucose is higher in WT compared to the KO mice
283 (**Figure 3C**). A significant interaction effect between female mice groups and time on blood
284 glucose level was found ($p = 0.0199$). As shown in **Figure 4C**, the general group effect on basal
285 blood glucose levels in male mice was significant for both control and high-fat diet groups.
286 Whereas, the general group effect on basal blood glucose levels in female mice fed control and
287 high-fat diet was not significant which shows that the effect on blood glucose levels might be
288 sexually dimorphic in *Nucb1* disrupted mice. No changes were observed for basal blood glucose
289 level of 60% fat-fed KO mice (**Figure 5C)**. Comprehensive GEE analysis showed when all
290 predictors (sex, age, diet, and mice groups) are gathered in the united data matrix, the general
291 effects of *Nucb1* genetic disruption (mice group) affected basal blood glucose significantly.

292 The results of GEE analysis of chow-fed mice and high fat-fed data are summarized in
293 ***Supplementary Table 3*** and ***Table 4***, respectively. As shown in ***Table 3***, the interaction of mice
294 sex, group, and age on weekly monitoring of chow-fed mice parameters was significant, indicating
295 the effect of genetic disruption of *Nucb1* on bodyweight, food intake and basal blood glucose level
296 of chow-fed mice is sex- and age-dependant. Moreover, the GEE analysis showed significant
297 general effects of sex, age, diet and mice group and various interaction combinations of these
298 predictors on weekly monitoring parameters in control and high-fat-fed mice (***Table 4***). These
299 results suggest sex-, age-, mice strain- and diet-specific effects when *Nucb1* is disrupted.

300 **3.3. Glucose tolerance tests (OGTT and IPGTT)**

301 *OGTT*

302 We determined whether the genetic disruption of *Nucb1* affects oral glucose handling in
303 mice. Blood glucose level was significantly lower at 30 min in male *Nucb1* KO mice after the oral
304 administration of 2g glucose/kg bodyweight compared to the littermate control group (**Figure 2E**).
305 Consistent with this result, the area under the curve (AUC) analysis shows that male *Nucb1* KO
306 mice handled blood glucose levels better during 20-60 min of the OGTT (**Figure 2H**). However,
307 this effect occurred in a sex-specific manner because no such effects were found in female *Nucb1*
308 KO mice, whose handling of blood glucose was not different from littermate controls (**Figure 3E**
309 and **Figure 3H**). The disruption of *Nucb1* did not affect blood glucose handling in high- fat-fed
310 mice of either sex after the oral administration of 2g glucose/kg bodyweight (**Figure 4F and**
311 **Figure 5F**). However, a reduced blood glucose level in female *Nucb1* KO mice fed control fat diet
312 at 10 min of OGTT was observed. The measurement of AUC for 10% fat-fed female mice
313 illustrates the same result during 0-20 min of OGTT (**Figure 5F** and **Figure 5I**). In addition, a
314 significant interaction between female mice group and time point was also observed ($p<0.0001$)
315 **(Figure 5F)**. In contrast, male *Nucb1* KO mice did not show significant changes in blood glucose
316 level when compared to WT littermates **(Figure 2C)**.

317 *IPGTT*

318 Male *Nucb1* KO mice had higher blood glucose level at 60 min after the IP administration
319 of glucose compared to WT littermate. Consistently, AUC measurement of showed higher value
320 during 30-90 min of IPGTT (**Figure 2F** and **Figure 2I**). In contrast, the genetic disruption of
321 *Nucb1* caused lower blood glucose levels in female mice at 20 min of IPGTT (**Figure 3F**).
322 However, the measurement of AUC illustrates the no significant difference between female WT
323 and KO during 10-30 min of IPGTT (**Figure 3I**). Moreover, male *Nucb1* KO mice fed control or
324 high-fat diets had lower blood glucose compared to WT during 30-120 min of IPGTT compared
325 to WT fed the same diets (**Figure 4J**). However, this difference in blood glucose was only
326 significant for male *Nucb1* KO mice at 120 min of IPGTT (**Figure 4G**). A significant general
327 effect of male mice group for both diets was detected. Besides, a significant interaction of mice
328 group and time point on blood glucose level was observed for male mice fed high-fat diet (**Figure**
329 **4G**). In contrast, female *Nucb1* KO mice fed control and high-fat diet did not reveal any significant

330 changes in blood glucose handling during IPGTT. A significant interaction (p=0.0105) was
331 observed for 10% fat-fed female mice (**Figure 5G**).

332 Overall, comprehensive GEE analysis on OGTT results of male and female mice fed a
333 chow diet showed that the glucose handling in the presence of *Nucb1* gene disruption occurs in a
334 sex- and time point-specific manner. Oral glucose handling in control and high-fat diet groups is
335 influenced by sex, fat percentage, time point and presence/absence of *Nucb1* disruption.

336 The general effect of time point and interaction of time point, sex, and mice group on blood
337 glucose handling in chow-fed mice got significant during IPGTT. The general effect of *Nucb1*
338 gene disruption (group), time point, sex, and fat percentage on blood glucose handling of mice fed
339 control and high-fat diet was detected as significant. Moreover, the different interactions of sex,
340 group, time point and diet in this group got significant. Although the comprehensive GEE analysis
341 did not demonstrate a significant general effect of *Nucb1* disruption on glucose handling during
342 OGTT and IPGTT except for high-fat-fed mice during IPGTT, it showed that the genetic
343 disruption of *Nucb1* affects glucose handling in a sex-, diet- and post-glucose administration time-
344 dependent manner (***Supplementary Tables 3 - 4***).

345 3.4. Assessment of whole-body energy homeostasis using comprehensive lab animal 346 monitoring system (CLAMS)

347 *Twenty-four-hour food intake*

348 In general, the disruption of *Nucb1* in male and female mice altered cumulative food intake,
349 which was found higher in KO mice when compared to littermate WT mice (p = 0.0392 and
350 0.0314, respectively) (**Figure 2G** and **Figure 3G**). Although this difference for male mice is more
351 evident during the dark phase (7 PM - 7 AM), a significant difference in food intake of male mice
352 was only found at the beginning of the light period (9 AM). In contrast, significant differences in
353 food intake of female mice were found between groups at different time points in both light and
354 dark phases. Due to time-specific responses, a significant interaction between mice groups and
355 time was observed on cumulative food intake in both sexes ($p < 0.0001$).

356 The genetic disruption of *Nucb1* altered food intake in males fed a control fat diet
357 (p=0.0177). A significant interaction on food intake was observed for these male mice with higher
358 food intake during the dark phase (**Figure 4H**). In contrast, no difference in food intake was

observed between male *Nucb1* KO and WT mice fed a high-fat diet during the light or dark phases (p=0.7248, **Figure 4H**). Food intake of female *Nucb1* KO mice fed both fat diets was similar to that of female WT mice. A significant interaction of mice group and time on food intake was only observed in female mice fed control (fat) diet (p=0.0463, **Figure 5H**).

Twenty-four-hour water intake

Cumulative water intake was significantly different among female groups at different time points of the dark phase (**Figure 3J**), being higher for *Nucb1* KO mice. However, no such differences were observed during the light period, and no general group effect was detected ($p = 0.2750$), but a significant interaction between group and time was found ($p < 0.0001$). The effect on water intake due to *Nucb1* disruption was sexually dimorphic due to *Nucb1* disruption because no significant differences were observed in cumulative water intake between groups in male mice (**Figure 2J**). Furthermore, water intake consumption in *Nucb1* KO mice were similar to that of WT mice of both sexes fed a control fat diet during light and dark phases. The cumulative water intake in female WT mice fed a high-fat diet was significantly higher during limited hours in the late light phase. However, no changes were found in male mice fed the same diet. A significant interaction between male mice groups fed the control fat diet and time on water intake was detected ($p<0.0001$), whereas such an interaction was not observed in female mice fed the same diet (**Figure 4K** and **Figure 5K**).

Twenty-four-hour physical activity

The disruption of *Nucb1* induced a significant increase in physical activity in male mice during the dark phase compared to WT littermates (**Figure 2K**). In contrast, physical activity in female mice displayed the opposite (decrease) of what was found with male mice in the dark phase (**Figure 3K**). Thus, here also, a sexually dimorphic effect was found due to the genetic disruption of *Nucb1*. Moreover, male, and female *Nucb1* KO mice fed control fat diet displayed similar results on physical activity (increase in male *Nucb1* KO and decrease in female *Nucb1* KO mice in dark phase) of what was found in chow-fed mice groups (**Figure 4L** and **Figure 5L**). These findings provide evidence on the sex-specific role of *Nucb1* disruption for physical activity when the fat percentage in diet is low. In contrast, high-fat-fed *Nucb1* KO mice did not show any significant physical activity compared to their WT littermates (**Figure 4L** and **Figure 5L**).

388 *Twenty-four-hour energy expenditure*

389 Our results indicate that male *Nucb1* KO mice fed chow diet had higher energy expenditure
390 (heat) than WT littermates in both light and dark phases (**Figure 2L**) but an increase in energy
391 expenditure in female *Nucb1* KO mice was found only during the light phase (**Figure 3L**). Energy
392 expenditure showed an increasing pattern during the light phase in male *Nucb1* KO mice fed 10%
393 fat while an opposite (decrease) effect in male KO groups fed high fat diet during the dark phase
394 (**Figure 4M**). In female mice, energy expenditure showed a decreasing pattern in KO groups fed
395 control fat diet in both phases, but an increasing pattern in those fed high fat diet in both phases
396 (**Figure 5M**).

397 *Twenty-four-hour energy derived from carbohydrates and fat*

398 Interestingly, our results demonstrate that the catabolism of neither carbohydrates (CHO)
399 nor fat was affected during the light phase between groups of either sex. The use of CHO in both
400 male and female *Nucb1* KO mice was increased in the dark phase while fat catabolism was reduced
401 compared to WT mice (**Figure 2L** and **Figure 3L**). The disruption of *Nucb1* decreased energy-
402 derived from fat and CHO in female mice fed control fat diets in both phases (**Figure 5M**). High
403 fat-fed male *Nucb1* KO mice had lower energy-derived from CHO during both phases, but female
404 KO mice displayed an increase in energy derived from CHO in both phases. Moreover, energy-
405 derived from fat was higher in female *Nucb1* KO mice in both phases, but in male KO mice was
406 lower only in dark phase (**Figure 4M** and **Figure 5M**).

407 Furthermore, GEE analysis showed the general effects of sex and age on weekly
408 monitoring of food intake and bodyweight in chow-fed mice were significant. The general effect
409 of sex on the weekly monitoring of basal blood glucose levels of chow-fed mice was also
410 significant. Moreover, the general effects of sex, age and diet on food intake and bodyweight were
411 significant. The general effect of *Nucb1* gene disruption on the weekly monitoring of blood glucose
412 of high-fat-fed mice were significant. Regarding the OGTT, the general effect of sex and time
413 point in chow-fed mice and the general effect of sex, time point and diet on oral blood glucose
414 handling were statistically significant. The general effects of all factors (sex, time group, *Nucb1*
415 disruption, diet) on IP glucose handling were significant for high-fat-fed mice.

416 GEE analysis of chow-fed mice data showed that the genetic disruption of *Nucb1* affected
417 cumulative food intake in mice, and the general effects of sex and/or dark/light phase for other
418 CLAMS parameters, including water intake, energy expenditure and total physical activity in the
419 mice fed the same diet were significant. Overall, the GEE analysis supports significant 3-way
420 interactions between the mice group, light phase, and mice sex on micro measurement of food
421 intake and water intake, energy expenditure and total physical activity in chow-fed mice. This
422 suggests that the genetic disruption of *Nucb1* affected whole-body energy metabolism of chow-
423 fed mice in a sex- and light phase-specific manner.

424 GEE analysis supports the results obtained from control and high-fat-fed mice, including
425 significant interactions between mice group, day phase, sex, and diet on CLAMS parameters. This
426 suggests that metabolic functions of obese mice were affected in *Nucb1* disrupted mice in a sex-,
427 diurnal phase- and diet-specific manner.

428 **3.5. Liver and adipose tissue weight**

429 Our results showed that although HSI was not different between both groups (i.e., WT and
430 *Nucb1* KO) in mice of either sex fed chow diet, WAT was higher in *Nucb1* KO mice in both sexes
431 (**Figure 2D** and **Figure 3D**). Like chow-fed mice results, the HSI index was unaffected by the
432 genetic disruption of *Nucb1* in control and high fat-fed male and female mice (**Figure 4E** and
433 **Figure 5E**). Unlike increased adiposity seen in both sexes of chow-fed KO mice, adiposity was
434 higher only in *Nucb1* disrupted male mice fed 60% fat diet (**Figure 4D)**.

435 **3.6. Metabolic gene expression in tissues of chow-fed mice**

436 As shown in **Figure 6**, the abundance of *preproghrelin* and *Nucb2* mRNAs in the stomach
437 of male *Nucb1* KO mice was increased, while no changes were observed in the female group
438 (**Figure 6B)**. In the duodenum, the *Gip* and *Glp-1* precursor mRNA levels were increased in female
439 *Nucb1* KO mice without any change in male mice (**Figure 6L)**. *Nucb2* abundance in the jejunum
440 of *Nucb1* KO mice showed a sex-specific pattern with a decrease in male KO and an increase in
441 female KO groups (**Figure 6G)**. *Ucp-1* mRNA in brown fat was enhanced in both sexes of *Nucb1*
442 KO mice (**Figure 6H)**. *Glut1*, *Glut2* and *Nucb2* mRNAs were unaffected by the disruption of
443 *Nucb1* in muscle samples.

4. Discussion

Our previous research identified biological roles for NUCB1-derived NLP, including feeding suppression and energy metabolism regulation in male rats [14], insulinotropic effects in MIN6 cells [10], and an anorectic effect in goldfish [11]. NUCB1/NLP co-localizes insulin in the pancreatic islet beta cells of mice [13]. The first goal of our research was to determine if the disruption of *Nucb1* affects whole-body energy homeostasis in mice. The disruption of *Nucb1* caused an increase in food intake in female mice fed a chow diet, but not in male mice, over a 24 h period. Chronic administration of NLP using osmotic minipumps over a 7-day period decreased day 3 and day 4 food intake, with normalization of feeding starting to appear from day 4 dark phase [14]. In the research presented here, while short-term adverse effects were found, the genetic disruption of *Nucb1* did not increase food intake and bodyweight gain in mice over a longer term (weekly monitoring for 5-6 months). This is likely due to adaptive responses to compensate for the absence of NUCB1 and normalize energy homeostasis, via changes including the upregulation of *Nucb2*. NESF-1, processed from NUCB2 that has a high analogy to NUCB1, exhibits an anorectic effect in rodents and modulates central and peripheral orexigenic and anorexigenic peptides [12]. NLP too affected metabolic regulatory hormone mRNA abundance in rats [14]. It is possible that the disruption of *Nucb1* influence the endocrine milieu, and this might indirectly affect energy balance.

In one report [20], *Nucb2* expression was not affected by age and/or diet in 3-month-old versus 6-month-old WT mice fed a high fat. In the same study, the ablation of *Nucb2* did not affect food intake or bodyweight in mice [20]. Although these results agree with our findings on weekly food intake monitoring, their short-term measurement of food intake for 72 h and one-time measurement of bodyweight (10-month-old mice) were different from our approaches, including continuous long-term monitoring. Moreover, several additional criteria, including two-way mixed ANOVA and GEE statistical analysis were employed here, which showed that the genetic disruption of *Nucb1* indeed affected food intake in a time-, diet- and sex-specific manner in high-fat-fed mice. Overall, the results from a very careful characterization with several factors included for consideration, the *Nucb1* disrupted mice exhibits mild perturbations in feeding.

The disruption of *Nucb1* in male and female mice did not alter basal blood glucose levels in weekly monitoring. Although solely based on *in vitro* studies, NLP was reported to stimulate

474 the secretion of insulin in MIN6 cells [10]. Based on this, we expected an elevation in blood
475 glucose due to the loss of positive effects of NLP on insulin synthesis and secretion from islet beta
476 cells. However, our results did not support this expected outcome. The development of
477 compensatory physiological responses, as mentioned earlier, might have contributed to this, as
478 well. Incretin hormones, including GLP-1 and GIP, are secreted by enteroendocrine cells in the
479 small intestine in response to ingested carbohydrates and are then responsible for the stimulation
480 of post-prandial insulin secretion [21]. Consistently, the level of incretin hormones at mRNA levels
481 were upregulated in *Nucb1* disrupted mice. OGTT and IPGTT are reference methods to assess how
482 oral or intraperitoneal delivery of glucose is handled by the organism. OGTT factors in the role of
483 intestinal incretin hormones. Opposite to what we expected, oral glucose handling was better in
484 male *Nucb1* KO mice fed chow diet, while no changes were not observed in female KO mice.
485 Similarly, the disruption of *Nucb1* improved IP glucose handling in male mice fed control and
486 high-fat diet. An increase in incretin hormone transcript abundance (*Gip* and *Glp-1 precursor*) was
487 found in female KO mice fed a chow diet, suggesting a possible role for incretins in the better
488 handling of glucose in *Nucb1* disrupted mice. Another reason for better normalization of glucose
489 following oral or intraperitoneal delivery is an increase in glucose uptake in the target tissues
490 (especially muscle, liver, and adipose tissue) [22] and changes in insulin sensitivity because of
491 genetic disruption of *Nucb1*. Besides, our lab has previously reported that the NESF-1-treated rats
492 had no effects on blood glucose levels, while it increased insulin, and decreased glucagon in rats
493 during an OGTT [23]. A positive effect for NESF-1 on gluconeogenesis in the liver was proposed
494 in that study based on gluconeogenic enzyme mRNA changes, as well as NESF-1 caused an
495 inhibition of glucose uptake in muscle [23]. If NESF-1 and NLP have similar positive effects in
496 increasing glucose in circulation, then the disruption of *Nucb1* would elicit the opposite effects. In
497 fact, our findings suggest that the genetic disruption of *Nucb1* improves insulin sensitivity, and
498 this could be due to a decrease in gluconeogenesis and an increase in glucose uptake.
499 Comprehensive GEE analysis demonstrated a significant general effect of group on blood glucose
500 handling during IPGTT for control and high-fat-fed mice, which supports our findings. Overall,
501 GEE analysis of OGTT and IPGTT results showed that *Nucb1* KO mice fed high-fat diet handled
502 blood glucose better in a sex-, diet- and time point-specific manner. Consistent with our findings,
503 global *Nucb2* deficient male mice fed high-fat diet normalized circulating blood glucose through
504 the increase of hepatic glucose uptake during glucose infusion to maintain euglycemia [20].

505 Considering the similarity between NESF-1 and NLP, the same effect could occur in *Nucb1*
506 disrupted mice when fed high-fat diet.

507 To determine whole-body energy homeostasis in *Nucb1* disrupted mice over a 24 h period,
508 CLAMS was used. An increase in food intake during the 24 h period in *Nucb1* disrupted mice was
509 found, but this was observed only in selected cohorts (chow-fed males and females and 10% fat
510 diet-fed male mice). This is a clear indication of how important nutrient composition is in such
511 studies. An increase in food intake of male *Nucb1* KO mice was associated with an increase in
512 preproghrelin (orexigen) mRNA abundance, which might be a contributing factor in the increased
513 food intake of male mice. Our unpublished results show that NESF-1 suppresses preproghrelin
514 mRNA in stomach endocrine cells. It is possible that NLP too regulates different short-term
515 appetite regulatory signals to elicits it effects in maintaining energy balance. This was indeed
516 evident in our sub-cutaneous infusion study in rats, where a number of metabolic regulators
517 mRNAs were found altered []. However, different compensatory physiological responses in the
518 multiple redundant milieu that regulates metabolism might have developed over a longer period
519 due to the genetic disruption of this peptide in mice. This could be a reason why we did not observe
520 major overall changes in the longer-term data in mice of both sexes.

521 Besides feeding, NUCB1/NLP and NUCB2/NESF-1 are implicated in the control of water
522 intake. Subcutaneous infusion of NLP over 7 days reduced water intake in male rats [14].
523 Meanwhile, intracerebroventricular (ICV) administration of NESF-1 decreased water intake in rats
524 [24]. This anti-dipsogenic effect was observed under water restriction or after a hypertonic
525 challenge. Interestingly, the anti-dipsogenic effect appeared to be dissociated from the
526 anorexigenic effect of NESF-1, as a higher dose of injected ICV was required for the reduction of
527 water intake. However, the injection of a lower dose of NESF-1 into the subfornical organ, a brain
528 structure that regulates fluid homeostasis, decreased food intake and potently increased water
529 intake in rats [24]. Our finding extends these observations that in the genetic disruption of *Nucb1*,
530 the cumulative water intake was significantly different among female groups at different time
531 points of the dark phase, being higher for KO mice fed chow diet. Since no differences were
532 observed during the light phase, no general group effect was detected ($p = 0.2705$), but a significant
533 interaction between factors was found ($p < 0.0001$). The impact on water intake due to *Nucb1*
534 disruption is sexually dimorphic as no significant differences were observed in cumulative water

535 intake of male mice. The diet composition might have affected water intake as no significant
536 changes was detected in WT and Nucb1 KO mice of both sexes fed high fat diet.

537 The subcutaneous infusion of NLP in male rats over 7 days decreased total physical activity
538 [14]. We observed that the genetic disruption of *Nucb1* induced a significant increase in physical
539 activity in male mice during the dark phase compared to WT littermates fed a chow diet and 10%
540 fat diet. In contrast, physical activity of female mice fed the same diets was opposite to what was
541 found in male mice in the dark phase. This is yet another sexually dimorphic effect for the genetic
542 disruption of *Nucb1*. The increased dark-phase physical activity might be due to the compensatory
543 response of NESF-1 in the genetic disruption of *Nucb1*. In fact, one study reported that central
544 administration of NESF-1 can cause hyperactivity which recovers to the normal level [25]. In
545 agreement with this finding, our lab previously found that long-term treatment of NESF-1 resulted
546 in increased physical activity on the seventh day of continuous infusion in rats [26]. NESF-1
547 expression was reported to be stimulated by alpha-melanocyte-stimulating hormone, which
548 triggers behaviours related to anxiety and fear, and possibly anxiety-mediated locomotor activity
549 [27]. Considering the observed mild phenotype in *Nucb1* KO mice, possibly due to the
550 compensatory response by NUCB2/NESF-1 and/or other factors, this potential explanation
551 supports our finding. However, this finding seems to be sexually dimorphic for the genetic
552 disruption of *Nucb.*

553 Energy balance is regulated by many factors that forms the endocrine and non-endocrine
554 milieu [28]. Previous studies reported that NLP and NESF-1 modulate whole-body energy
555 hemostasis in rats [14, 30]. Male *Nucb1* KO mice fed chow diet exhibited higher energy
556 expenditure (heat) than WT littermates in both light and dark phases, but an increase in energy
557 expenditure in female *Nucb1* KO mice applied only in the light phase suggesting energy balance
558 was affected at time-specific manner. This increase was associated with an increase in *Ucp-1*
559 mRNA level in the brown fat of these mice. NLP infusion in rats upregulated *Ucp-1* abundance
560 and increased thermogenesis which might be a reason for the elevation of energy expenditure.
561 However, the increased energy expenditure in *Nucb1* disrupted mice could be at least partly
562 attributed to the compensatory upregulation of NESF-1 that has a stimulatory role on *Ucp-1*
563 expression. The substrate utilization for energy expenditure was also investigated in this research.
564 The infusion of NLP in rats reduced energy derived from fat while carbohydrate catabolism was

565 unaffected for 7 days [14]. Consistent with previous observations, NESF-1-treated rats used fat as
566 a primary source of energy [29]. While these are pharmacological studies based on testing a single
567 dose of the peptide or one mode of administration, direct comparisons of such studies and genetic
568 loss are not always precise. However, these findings provide further evidence to support the fact
569 that both NLP and NESF-1 are fat- influencing peptides, and during their absence, energy derived
570 from fat might alter. The results presented here demonstrate that the catabolism of neither CHO
571 nor fat was altered during the light phase in both sexes fed chow diet, and the use of CHO by KO
572 male and female mice was increased in the dark phase while lipid catabolism was reduced
573 compared to WT mice. The catabolism of CHO decreased in male *Nucb1* KO mice but enhanced
574 in female KO fed high-fat diet mice during both phases. This suggests that the substrate selection
575 for energy production depends on sex and diet ingredients, and the overall compensatory changes
576 due to *Nucb1* disruption affect substrate utilization in these mice. It is also important to note that
577 observed phenotype for *Nucb1* gene disruption may also be dependent on the species studied.

578 Metabolic tissue weights were also measured in this research. Although HSI was not
579 different between groups (i.e., WT and *Nucb1* KO) in both sexes for all diets, WAT was higher in
580 *Nucb1* KO mice in both sexes fed chow diet and in male KO mice fed high-fat diet. NUCB2/NESF-
581 1 was earlier reported to suppress adipocyte differentiation in the mouse preadipocyte cells (3T3-
582 L1 cells) [30]. NESF-1 has been known as a novel-depot-specific adipokine that has a role in
583 reducing fat mass [31]. Consistently our lab previously reported that the expression of leptin
584 mRNA was reduced in WAT of NLP-treated rats, while the level of adiponectin and resistin
585 mRNA were elevated [14]. These results support our previous findings that NLP is a fat-
586 influencing protein in sex- and diet-specific manner. While some changes in tissue weights were
587 found in selected groups of mice, no major differences in bodyweight were detected in *Nucb1*
588 disrupted mice in comparison to WT litters. Since the pattern of bodyweight gain was different in
589 60% fat fed male *Nucb1* KO mice versus WT littermates, a significant interaction between male
590 mice and time was observed in bodyweight gain ($p < 0.0001$). Together, we did not find any major
591 changes in bodyweight due to the disruption of *Nucb1*.

592 **5. Conclusions**

593 The results of this research provide some supportive evidence for the importance of
594 endogenous *Nucb1*. While it is not critical for growth and reproduction, a mild metabolic

595 phenotype was observed. It is also acknowledged that these effects were found even in the presence
596 of possible compensatory changes in NUCB2/NESF-1, which has structural and functional
597 similarities with *Nucb1*. Another point to note is that the phenotype observed is significant
598 compared to the null phenotype found when more traditional endocrine regulators of metabolism
599 are disrupted or removed [32]. An important finding of our work lies in the interactions observed
600 and highlights the importance of considering the sex, diet and other parameters when interpreting
601 and concluding on research results from KO mice. The reasons for sexual dimorphism found in
602 this research remain unknown, and it clearly is an important topic for follow-up research. The
603 reasons for sexual dimorphism in the mice are also very interesting, and future studies should
604 consider some lines of research in this field.

605

6. Acknowledgments

The authors thank Dr. Sarah Parker, Statistician, WCVM for her kind assistance with our study design and statistical analysis.

7. Funding Source

This research was supported by a project grant from the Canadian Institutes of Health Research (CIHR), and funding from the University of Saskatchewan through the Centennial Enhancement Chair in Comparative Endocrinology to SU. Infrastructure support for the project was provided by John Evans Leader's Fund grant from the Canada Foundation of Innovation (CFI) and an Establishment Grant from the Saskatchewan Foundation of Health Research (SHRF) to SU. AN and JJR were supported by Dean's scholarships from the University of Saskatchewan. E.J.V. was supported by a postdoctoral fellowship (#4530) and a Top-Up Incentive Award (#5362) from the Saskatchewan Health Research Foundation (SHRF), and a postdoctoral fellowship (#2019MFE-429976-71377) from the Canadian Institutes of Health Research (CIHR). AH was a recipient of the CIHR post-doctoral fellowship.

8. Data availability

The data of this study are available from the corresponding author upon reasonable request.

9. Supplementary material

Supplementary information are available as separate document.

10. Role of co-authors

AN and E.J.V. planned and performed the experiments, analyzed the data, and prepared the manuscript. J.J.R helped in performing some experiments using high-fat-fed mice. AH established and optimized genotyping technique. SU provided the original ideas, funding for this research, helped design experiments and interpretation of the results, and manuscript review and editing. All authors read and approved the final manuscript.

11. References

[1] Leung AK-W, Ramesh N, Vogel C, Unniappan S. Nucleobindins and encoded peptides: From cell signaling to physiology. Advances in protein chemistry and structural biology. 2019;116:91-133.

[2] Miura K, Titani K, Kurosawa Y, Kanai Y. Molecular cloning of nucleobindin, a novel DNA-binding protein that contains both a signal peptide and a leucine zipper structure. Biochemical and biophysical research communications. 1992;187:375-80.

[3] Kanai Y, Katagiri T, Mori S, Kubota T. An established MRL/Mp-lpr/lpr cell line with null cell properties produces a B cell differentiation factor (s) that promotes anti-single-stranded DNA antibody production in MRL spleen cell culture. International Archives of Allergy and Immunology. 1986;81:92-4.

[4] Kanai Y, Isonishi S, Katagiri T, Koizumi T, Miura K, Kurosawa Y. Early induction of anti-double-stranded DNA antibodies in lupus-prone MRL mice inoculated with Ly-24+ cells cloned from lymph node cells of an MRL/Mp-lpr/lpr mouse: possible effect of putative cytokines produced by cloned Ly-24+ cells. Immunology letters. 1990;24:49-55.

[5] Stengel A, Goebel M, Yakubov I, Wang L, Witcher D, Coskun T, et al. Identification and characterization of nesfatin-1 immunoreactivity in endocrine cell types of the rat gastric oxyntic mucosa. Endocrinology. 2009;150:232-8.

[6] Williams P, Tulke S, Ilegems E, Berggren P-O, Broberger C. Expression of nucleobindin 1 (NUCB1) in pancreatic islets and other endocrine tissues. Cell and tissue research. 2014;358:331-42.

[7] Balasubramanian V, Srinivasan B. Genetic analyses uncover pleiotropic compensatory roles for Drosophila Nucleobindin-1 in inositol trisphosphate-mediated intracellular calcium homeostasis. Genome. 2020;63:61-90.

[8] Williams P. Investigations into the Distribution and Function of Nucleobindin 1: Karolinska Institutet (Sweden); 2019.

[9] Tulke S, Williams P, Hellysaz A, Ilegems E, Wendel M, Broberger C. Nucleobindin 1 (NUCB1) is a Golgi-resident marker of neurons. Neuroscience. 2016;314:179-88.

[10] Ramesh N, Mohan H, Unniappan S. Nucleobindin-1 encodes a nesfatin-1-like peptide that stimulates insulin secretion. General and comparative endocrinology. 2015;216:182-9.

[11] Sundarrajan L, Blanco AM, Bertucci JI, Ramesh N, Canosa LF, Unniappan S. Nesfatin-1-like peptide encoded in nucleobindin-1 in goldfish is a novel anorexigen modulated by sex steroids, macronutrients and daily rhythm. Scientific reports. 2016;6:1-14.

[12] Oh-I S, Shimizu H, Satoh T, Okada S, Adachi S, Inoue K, et al. Identification of nesfatin-1 as a satiety molecule in the hypothalamus. Nature. 2006;443:709-12.

[13] Ramesh N. Nesfatin-1 and Nesfatin-1-Like Peptide (NLP) Regulation of Energy Balance in Mice: University of Saskatchewan; 2019.

[14] Gawli K, Ramesh N, Unniappan S. Nesfatin-1-like peptide is a novel metabolic factor that suppresses feeding, and regulates whole-body energy homeostasis in male Wistar rats. Plos one. 2017;12:e0178329.

[15] Vélez EJ, Nasri A, Unniappan S. Nesfatin-1 and Nesfatin-1-like peptide suppress basal and TRH-Induced expression of prolactin and prolactin regulatory element-binding protein mRNAs in rat GH3 somatolactotrophs. Molecular and Cellular Endocrinology. 2021;529:111269.

676 [16] Vélez EJ, Unniappan S. Nesfatin-1 and nesfatin-1-like peptide suppress growth hormone
677 synthesis via the AC/PKA/CREB pathway in mammalian somatotrophs. Scientific reports.
678 2020;10:1-12.
679 [17] McLean J, Tobin G. Animal and human calorimetry: Cambridge University Press; 2007.
680 [18] Nasri A, Unniappan S. Nucleobindin-derived nesfatin-1 and nesfatin-1-like peptide
681 stimulate pro-opiomelanocortin synthesis in murine AtT-20 corticotrophs through the
682 cAMP/PKA/CREB signaling pathway. Molecular and Cellular Endocrinology.
683 2021;536:111401.
684 [19] Maxwell SE, Delaney HD, Kelley K. Designing experiments and analyzing data: A model
685 comparison perspective: Routledge; 2017.
686 [20] Ravussin A, Youm Y-H, Sander J, Ryu S, Nguyen K, Varela L, et al. Loss of nucleobindin-
687 2 causes insulin resistance in obesity without impacting satiety or adiposity. Cell reports.
688 2018;24:1085-92. e6.
689 2[21] Kazakos K. Incretin Effect: Glp-1, Gip, Dpp4. Diabetes research and clinical practice.
690 2011;93:S32-S6.
691 [22] Shi J, Kandror KV. Study of glucose uptake in adipose cells. Adipose tissue protocols:
692 Springer; 2008. p. 307-15.
693 [23] Gonzalez R, Perry R, Gao X, Gaidhu M, Tsushima R, Ceddia R, et al. Nutrient responsive
694 nesfatin-1 regulates energy balance and induces glucose-stimulated insulin secretion in rats.
695 Endocrinology. 2011;152:3628-37.
696 [24] Yosten G, Redlinger L, Samson W. Evidence for a role of endogenous nesfatin-1 in the
697 control of water drinking. Journal of neuroendocrinology. 2012;24:1078-84.
698 [25] Yosten GL, Samson WK. Nesfatin-1 exerts cardiovascular actions in brain: possible
699 interaction with the central melanocortin system. American Journal of Physiology-Regulatory,
700 Integrative and Comparative Physiology. 2009;297:R330-R6.
701 [26] Mortazavi S, Gonzalez R, Ceddia R, Unniappan S. Long-term infusion of nesfatin-1 causes
702 a sustained regulation of whole-body energy homeostasis of male Fischer 344 rats. Frontiers in
703 cell and developmental biology. 2015;3:22.
704 [27] Merali Z, Cayer C, Kent P, Anisman H. Nesfatin-1 increases anxiety-and fear-related
705 behaviors in the rat. Psychopharmacology. 2008;201:115-23.
706 [28] Pasiakos SM, Caruso CM, Kellogg MD, Kramer FM, Lieberman HR. Appetite and
707 Endocrine Regulators of Energy Balance After 2 Days of Energy Restriction: Insulin, Leptin,
708 Ghrelin, and DHEA-S. Obesity. 2011;19:1124-30.
709 [29] Mohan H, Ramesh N, Mortazavi S, Le A, Iwakura H, Unniappan S. Nutrients differentially
710 regulate nucleobindin-2/nesfatin-1 in vitro in cultured stomach ghrelinoma (MGN3-1) cells and
711 in vivo in male mice. PLoS One. 2014;9:e115102.
712 [30] Tagaya Y, Osaki A, Miura A, Okada S, Ohshima K, Hashimoto K, et al. Secreted
713 nucleobindin-2 inhibits 3T3-L1 adipocyte differentiation. Protein and Peptide Letters.
714 2012;19:997-1004.
715 [31] Dong J, Xu H, Xu H, Wang P-f, Cai G-j, Song H-f, et al. Nesfatin-1 stimulates fatty-acid
716 oxidation by activating AMP-activated protein kinase in STZ-induced type 2 diabetic mice.
717 PLoS One. 2013;8:e83397.
718 [32] Lin S, Boey D, Herzog H. NPY and Y receptors: lessons from transgenic and knockout
719 models. Neuropeptides. 2004;38:189-200.

720

721 **Figure Legends:**

722 **Figure 1.** RT-PCR analysis of tail (A), intestine (B) and pancreas (C) to confirm the disruption of
723 *Nucb1* gene in *Nucb1* KO mice and to compare it with WT mice. The band corresponding to 397
724 bp shows the disruption of *Nucb1* in mice and band corresponding to 611 bp shows intact *Nucb1*
725 gene in WT mice.

726 **Figure 2**. General characterization of chow-fed male WT and *Nucb1* KO mice. Normal
727 distribution of the data, the homogeneity of variances and covariances were determined using
728 Shapiro-Wilk test, Levene's test, and Box's test, respectively. The two-way mixed ANOVA was
729 performed. A Bonferroni's multiple comparison test was also performed as a post hoc analysis to
730 compare the dependent variable results between mice strain (group) in each time point. Unpaired
731 t-test was used for analyzing the differences in energy expenditure, energy derived from
732 carbohydrates or fat and total physical activity in CLAMS studies, as well as to compare AUC in
733 the glucose tolerance tests (IPGTT and OGTT). All the analyses were carried out using GraphPad
734 Prism 8.0, and statistical differences were considered at $p < 0.05$. The number of mice in each of
735 the experiments is provided below: Weekly tracking: WT n = 7; KO n = 12, CLAMS: n = 6-8
736 mice/group/sex (20-21 weeks old), Glucose tolerance tests (GTTs): WT n = 7; KO n = 10-12

737 **Figure 3**. General characterization of chow-fed female WT and *Nucb1* KO mice. Normal
738 distribution of the data, the homogeneity of variances and covariances were determined using
739 Shapiro-Wilk test, Levene's test, and Box's test, respectively. The two-way mixed ANOVA was
740 performed. A Bonferroni's multiple comparison test was also performed as a post hoc analysis to
741 compare the dependent variable results between mice strain (group) in each time point. Unpaired
742 t-test was used for analyzing the differences in energy expenditure, energy derived from
743 carbohydrates or fat and total physical activity in CLAMS studies, as well as to compare AUC in
744 the glucose tolerance tests (IPGTT and OGTT). All the analyses were carried out using GraphPad
745 Prism 8.0, and statistical differences were considered at $p < 0.05$. The number of mice in each of
746 the experiments is provided below: Weekly tracking: WT n = 7-8; KO n = 8-12, n was varied due
747 to variation in sample size for some weeks, CLAMS: n = 6-8 mice/group/sex (20-21 weeks old),
748 Glucose tolerance tests (GTTs): WT n = 6; KO n = 7

749 **Figure 4.** General characterization of control and high-fat-fed male WT and *Nucb1* KO mice.
750 Normal distribution of the data, the homogeneity of variances and covariances were determined
751 using Shapiro-Wilk test, Levene's test, and Box's test, respectively. The two-way mixed ANOVA
752 was performed. A Bonferroni's multiple comparison test was also performed as a post hoc analysis
753 to compare the dependent variable results between mice strain (group) in each time point. Unpaired
754 t-test was used for analyzing the differences in energy expenditure, energy derived from
755 carbohydrates or fat and total physical activity in CLAMS studies, as well as to compare AUC in
756 the glucose tolerance tests (IPGTT and OGTT). All the analyses were carried out using GraphPad
757 Prism 8.0, and statistical differences were considered at $p < 0.05$. The number of mice in each of
758 the experiments is provided below: Weekly tracking: 10% fat fed mice WT n = 10-12; KO n = 10-
759 14, 60% fat fed mice WT n = 9-11; KO n = 10-13n was varied due to variation in sample size for

some weeks, CLAMS10% fat fed mice WT n = 6-8; KO n = 6-9, 60% fat fed mice WT n = 6-7; KO n = 8-9 mice/group/sex (28-29 weeks old), Glucose tolerance tests (GTTs): 10% fat fed mice WT n =12 ; KO n = 10-11, 60% fat fed mice WT n = 8; KO n = 13

Figure 5. General characterization of control and high-fat-fed female WT and *Nucb1* KO mice. Normal distribution of the data, the homogeneity of variances and covariances were determined using Shapiro-Wilk test, Levene's test, and Box's test, respectively. The two-way mixed ANOVA was performed. A Bonferroni's multiple comparison test was also performed as a post hoc analysis to compare the dependent variable results between mice strain (group) in each time point. Unpaired t-test was used for analyzing the differences in energy expenditure, energy derived from carbohydrates or fat and total physical activity in CLAMS studies, as well as to compare AUC in the glucose tolerance tests (IPGTT and OGTT). All the analyses were carried out using GraphPad Prism 8.0, and statistical differences were considered at $p < 0.05$. The number of mice in each of the experiments is provided below: Weekly tracking: 10% fat fed mice WT n = 9-10 ; KO n = 11-15, 60% fat fed mice WT n = 10-11; KO n = 12-14 n was varied due to variation in sample size for some weeks, CLAMS10% fat fed mice WT n = 6-8; KO n = 7-9, 60% fat fed mice WT n = 6-7; KO n = 7-8 mice/group/sex (28-29 weeks old), Glucose tolerance tests (GTTs): 10% fat fed mice WT n = 10; KO n = 14, 60% fat fed mice WT n = 11; KO n = 14

Figure 6. Metabolic gene expression of tissues obtained from *Nucb1* KO mice fed chow diet. The number of samples: >8 tissues/ group/sex. Asterisks show significant differences between WT and KO groups.

Nasri et al.
FIGURE 1

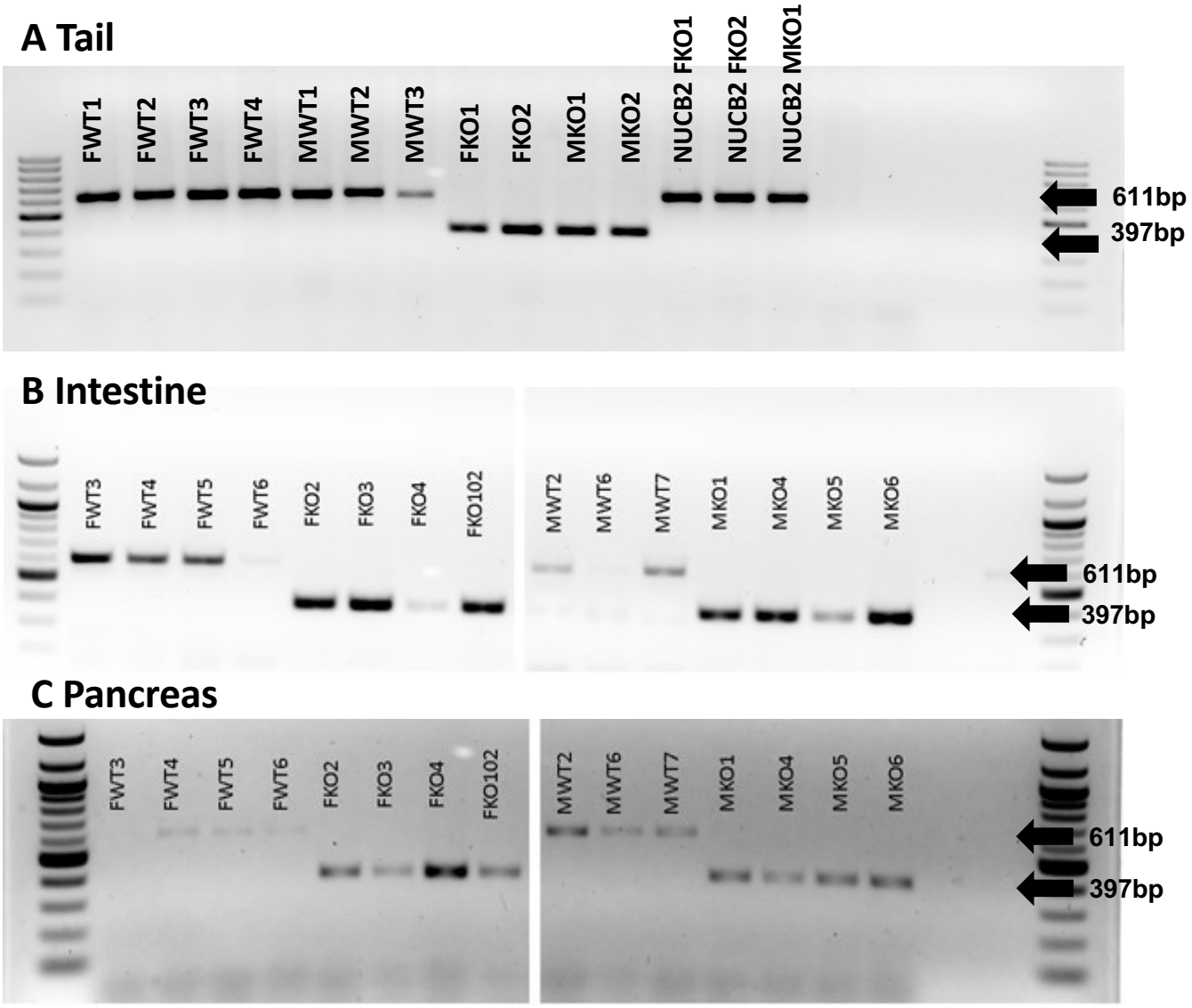

FIGURE 2
Nasri et al.

MALES (Chow Diet)

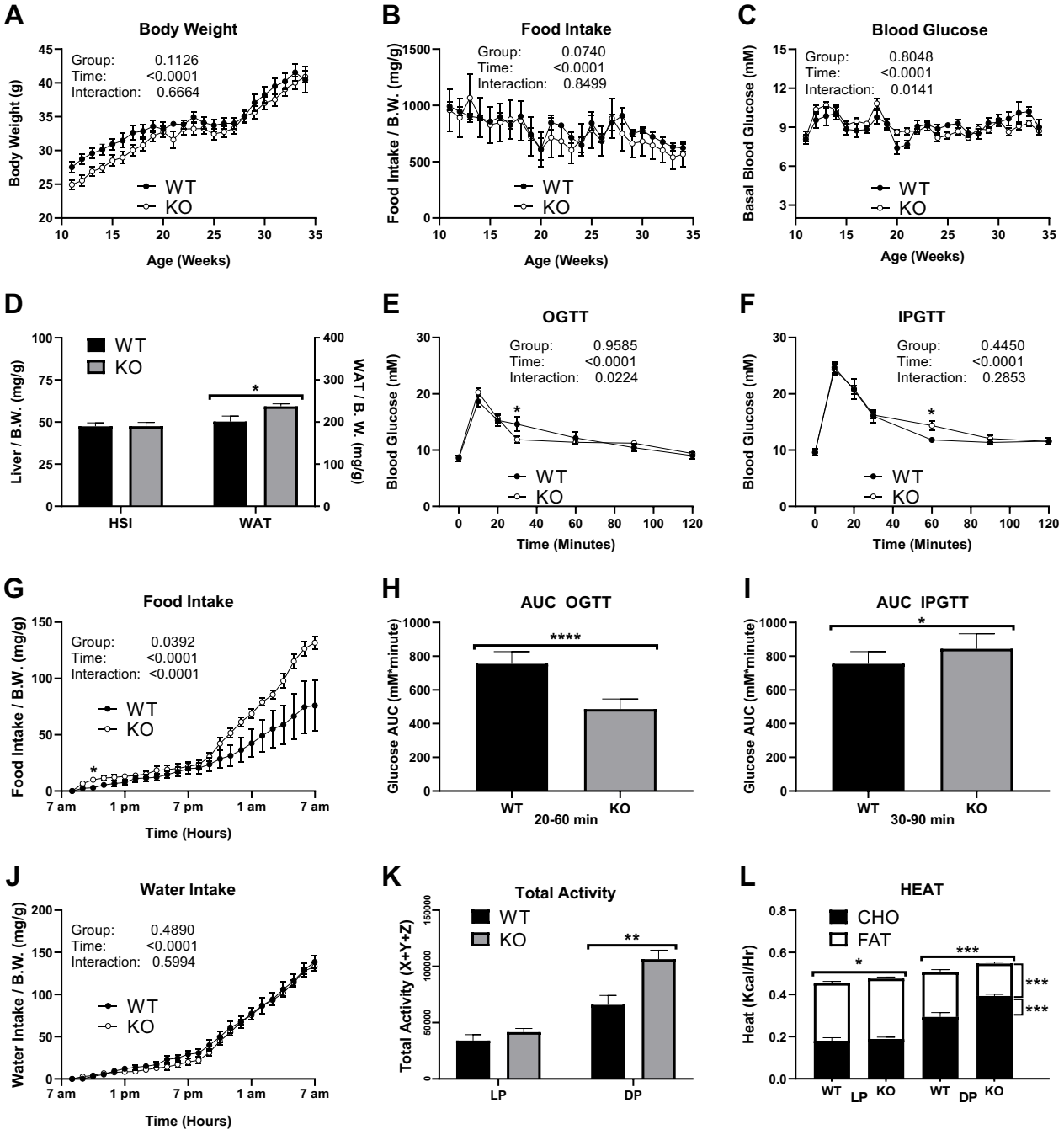

FIGURE 3
Nasri et al.

FEMALES (Chow Diet)

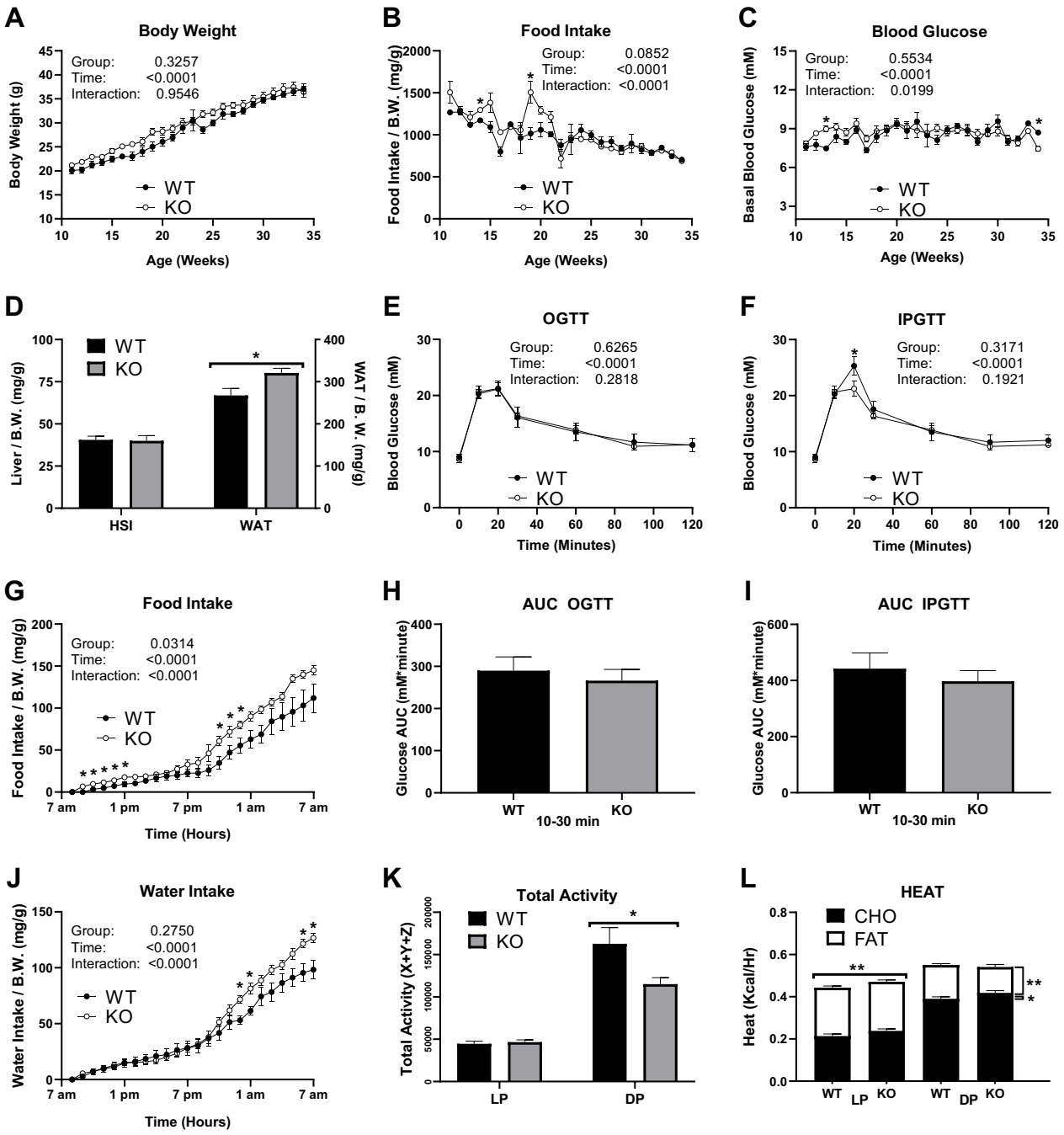

FIGURE 4
Nasri et al.

MALES (High Fat Diet)

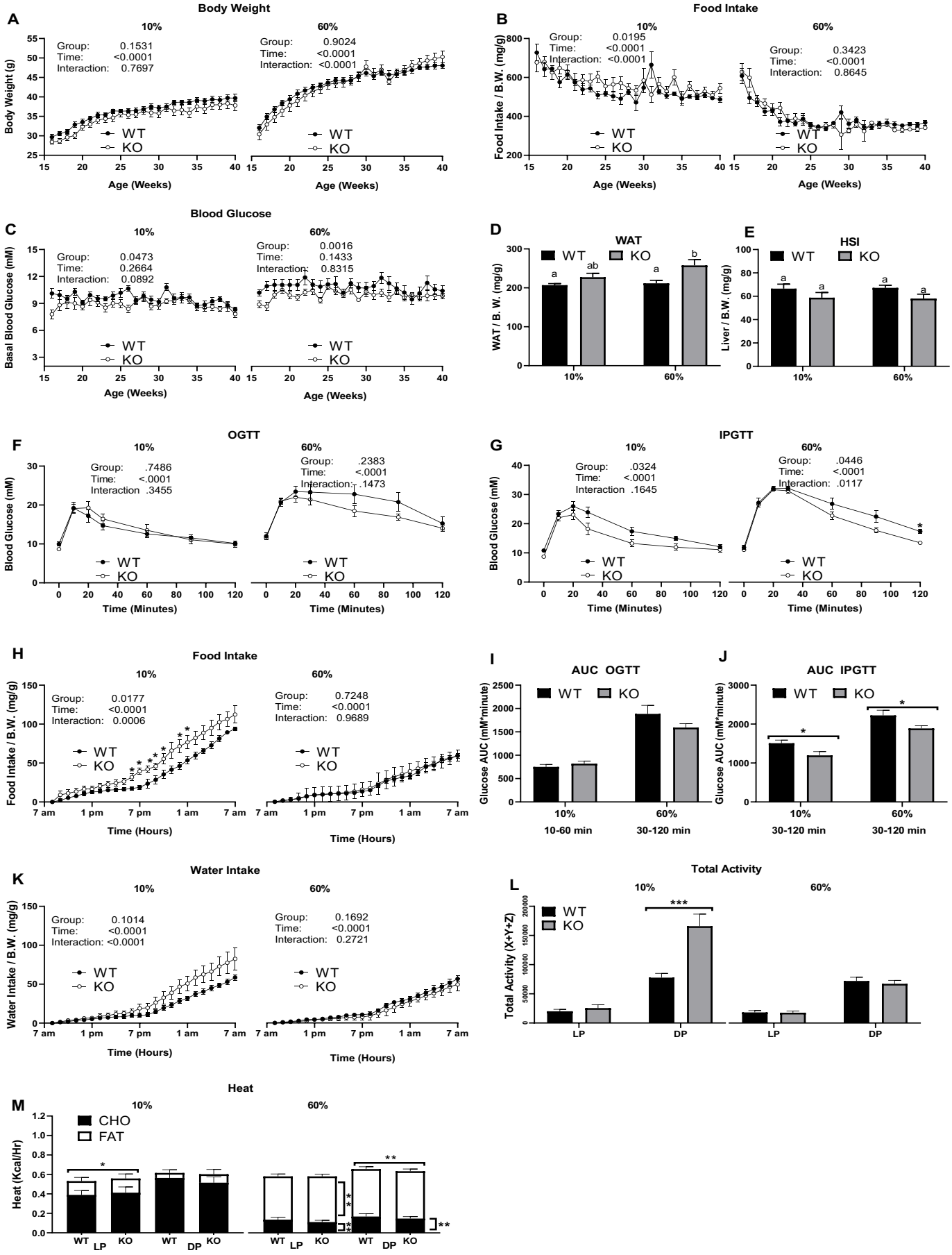

FEMALES (High Fat Diet)

FIGURE 5
Nasri et al.

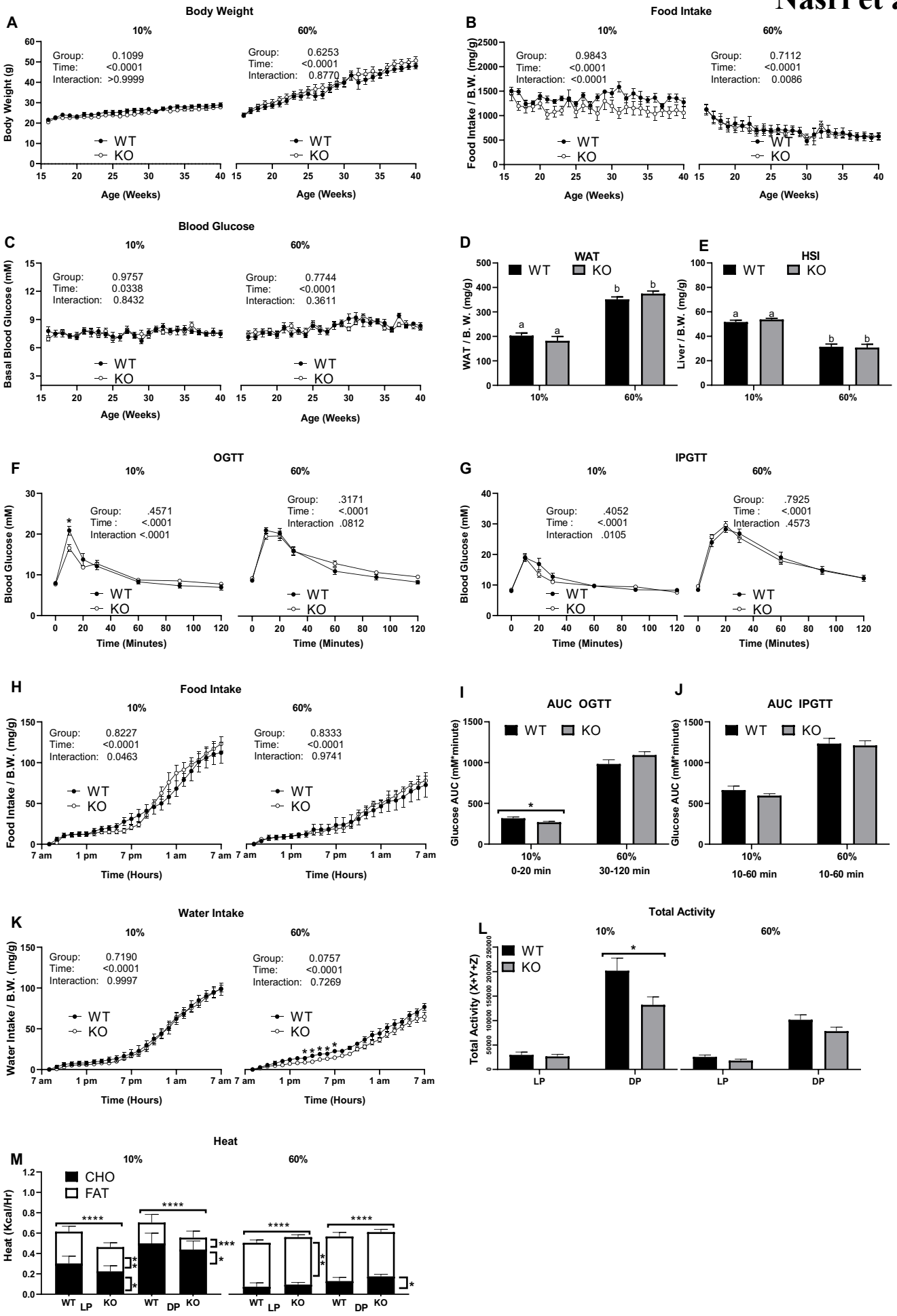

MALES AND FEMALES (CHOW DIET) FIGURE 6
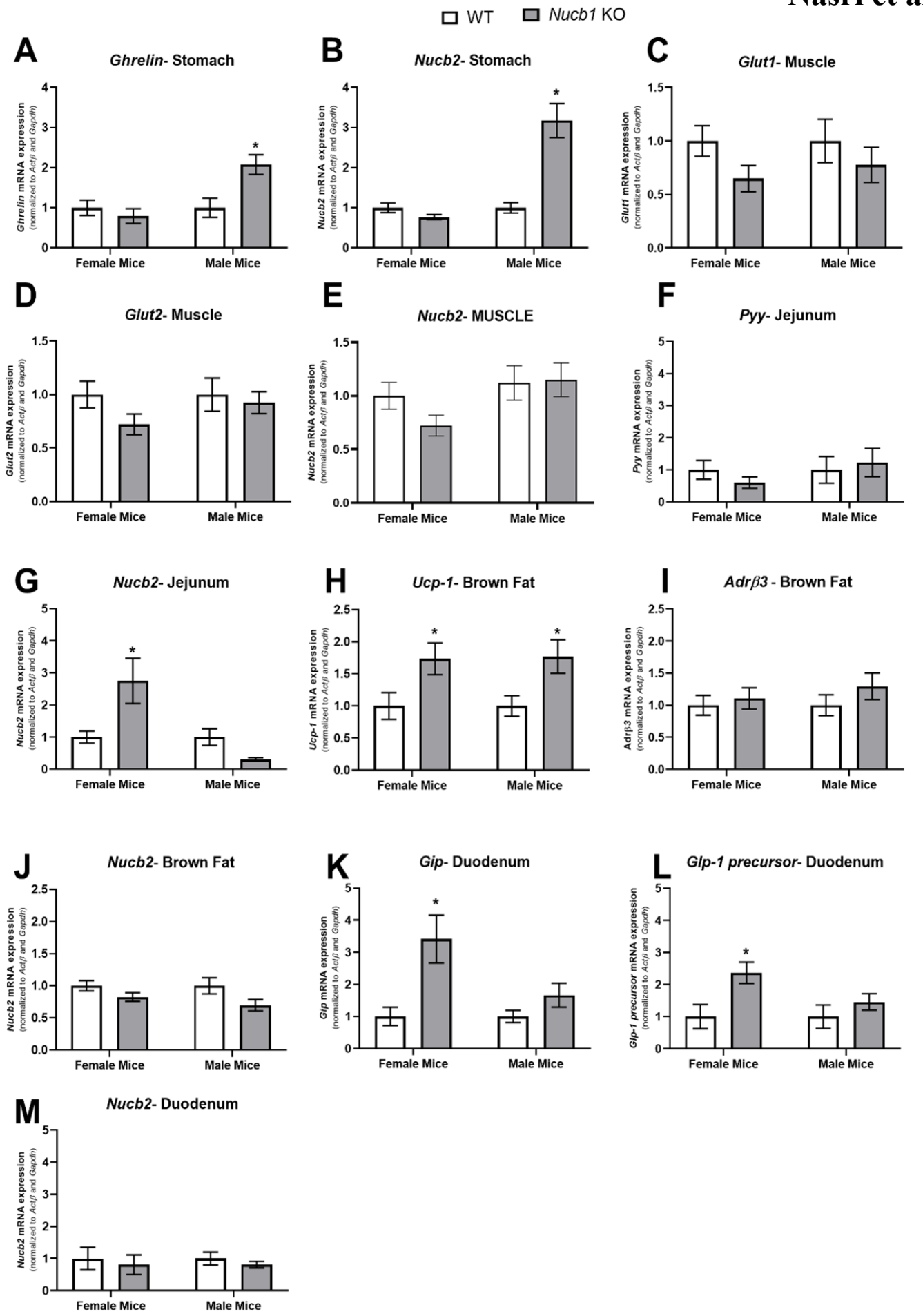
Nasri et al.